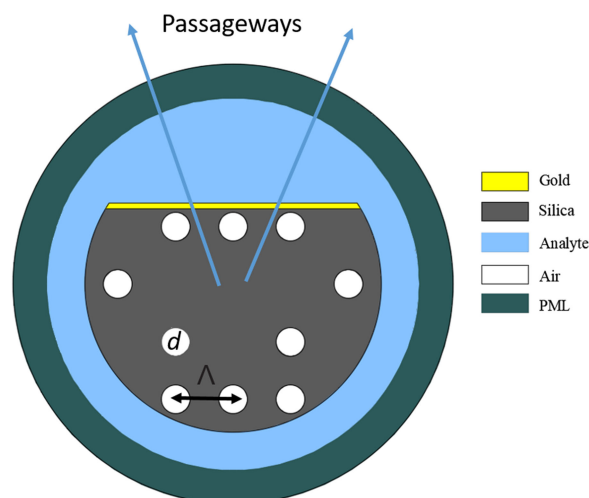


Highly Sensitive D-Shaped Plasmonic Refractive Index Sensor for a Broad Range of Refractive Index Detection

Volume 13, Number 1, February 2021



Emranul Haque
Abdullah Al Noman, *Graduate Student Member, IEEE*
Md. Anwar Hossain, *Senior Member, IEEE*
Nguyen Hoang Hai, *Member, IEEE*
Yoshinori Namihira, *Life Member, IEEE*
Feroz Ahmed, *Member, IEEE*



DOI: 10.1109/JPHOT.2021.3055234

Highly Sensitive D-Shaped Plasmonic Refractive Index Sensor for a Broad Range of Refractive Index Detection

Emranul Haque ¹

Abdullah Al Noman,¹ *Graduate Student Member, IEEE*,
Md. Anwar Hossain ², *Senior Member, IEEE*, Nguyen Hoang
Hai,³ *Member, IEEE*, Yoshinori Namihira,⁴ *Life Member, IEEE*,
and Feroz Ahmed ¹, *Member, IEEE*

¹Department of Electrical and Electronic Engineering, Independent University 1230, Bangladesh

²Department of Electrical and Electronic Engineering, Bangladesh University of Business and Technology (BUBT), Dhaka 1216, Bangladesh

³School of Electronics and Telecommunication, Hanoi University of Science and Technology, Thanh Xuan District, Hanoi 100000, Vietnam

⁴Professor Emeritus of University of the Ryukyus, Okinawa 903-0213, Japan

DOI:10.1109/JPHOT.2021.3055234

This work is licensed under a Creative Commons Attribution 4.0 License. For more information, see <https://creativecommons.org/licenses/by/4.0/>

Manuscript received November 11, 2020; revised January 4, 2021; accepted January 25, 2021. Date of publication January 29, 2021; date of current version February 15, 2021. Corresponding author: Emranul Haque (e-mail: emran1612@iub.edu.bd).

Abstract: In this paper, an extremely sensitive Photonic Crystal Fiber (PCF) based Surface Plasmon Resonance (SPR) sensor having D-shaped structure has been proposed. Gold has been used as the plasmonic material, and it has been coated outside of the fiber on its glassy surface to detect the change in the refractive index of the surrounding medium. Gold has been chosen as it is chemically stable and has no impact on the surrounding aqueous medium. Maximum Wavelength Sensitivity (WS) of 216,000 nm/RIU and Amplitude Sensitivity (AS) of 1680 RIU⁻¹ have been achieved for the analyte refractive index range 1.23 to 1.42 by the proposed sensor. After conducting a detailed literature review in the relevant field, it has been revealed that the proposed sensor possesses the highest wavelength sensitivity among recently reported PCF-SPR sensors to this date. The proposed sensor also exhibits a resolution of 4.63×10^{-7} RIU and FOM of 1200. Consequently, the proposed sensor can become an ideal candidate in the field of biomedical sensing, chemical sensing, and other lower RI analytes sensing.

Index Terms: Surface plasmon resonance, photonic crystal fiber, refractive index.

1. Introduction

Surface Plasmon Resonance (SPR) is the phenomenon explained in optics, which is the vibration of the electrons that are not associated with a single atom in a molecule, ion, or solid metal. In the Photonic Crystal Fiber (PCF) based SPR sensor, this vibration generally takes part in the metal-dielectric interface. It generates surface plasmonic waves that travel into the interface known as Surface Plasmon Polariton (SPP) [1]. The densely charged particles of the various plasmonic materials produce SPPs. Surface Plasmons in the PCF-SPR sensor are immensely sensitive to the

RI of the surrounding medium. When the plasmonic mode and the fundamental mode intersect with each other, SPR occurs, which is also defined as a phase-matching point. This leads the PCF-SPR sensor to detect the wavelength shifting as well as to sense the RI changes of the analyte of the surrounding medium. PCF-SPR sensor has gained popularity over the conventional SPR sensor as the conventional sensors' structural design is based on V-groove waveguide, slot wavelength, prism, which is very bulky and costly [2]. On the other hand, PCF-SPR sensors are very compact, cheap, and its features of the microscale application, label-free detection, ease of fabrication, etc. have gained more attention from the researchers in this field [2], [3].

The primary motive for designing the PCF-SPR sensor is to achieve maximum coupling efficiency between the fundamental mode and plasmonic mode by optimizing the structural parameters such as air hole ring lattice setting, diameters of the air holes, pitch, selection of plasmonic material, etc. of the PCF-SPR sensor [4]. Various types of structures, including long-period Bragg grating, microfluidic slot-based constructions, interior metal-coated, outer metal-coated, D-shaped formation, and so on, have been studied and analyzed for numerous PCF-SPR based detection applications [5]. Generally, two types of sensing technic are implied in PCF-SPR sensors. One is the internal sensing mechanism, and the other is the mechanism associated with sensing externally. The composition having an internal sensing mechanism where metal coated on the air holes' outer surface in the cladding region has been studied and analyzed, demonstrating a significant result of great sensitivity for practical application [3], [5]. Internally coated SPR sensors have selectively filled analyte channels that decrease the fabrication feasibility. The scheme of filling and vacating these channels with the analyte is challenging and time-consuming [5]. To address the challenging issues and drawbacks of internal metal-coated PCF-SPR, the external sensing mechanism-based D-shaped PCF-SPR structure has been demonstrated, which possess WS of 2900 nm/RIU [6]. A modified D-shaped PCF structure has been proposed to increase the spectral sensitivity. The plasmonic material is coated on an open ring analyte channel, and the achieved WS is 20000 nm/RIU [7].

The sensing performance of the PCF-SPR sensor is very much influenced by the selection of plasmonic materials [5], [7]. In this regard, gold and silver are mostly considered for designing the PCF-SPR sensor. Gold is also preferred over silver as it is chemically stable for a longer period, oxidation of the metal film is highly unlikely, and it displays greater resonance peak shifts [8]. However, silver shows a sharper resonance peak with respect to other plasmonic metals, and its chemical instability can be minimized by adding an adhesive agent such as TiO_2 [9]. For analyte sensing range 1.33 to 1.43, the maximum WS of 46000 nm/RIU has been reported where gold is used as plasmonic material [10]. Various PCF based SPR sensors which have been competent to detect the refractive index of analyte starting with 1.33 have been demonstrated in [5]–[15]. Nowadays, essential applications are arising where the lower refractive indexes (less than 1.3) are needed to be detected [16], and a small number of studies have been with the PCF-SPR sensor that could sense the RI less than 1.3 [3]. Some of the PCF-SPR sensors capable of detecting RI lower than 1.3 are proposed in [16]–[21], and their maximum achieved WS are 11055, 13000, 13500, 51000, and 116000 nm/RIU, respectively.

In this work, a D-shaped PCF based SPR sensor has been proposed and numerically investigated for wide range of RI (1.23-1.42) detection. Gold has been chosen as the plasmonic material for this design as it has no impact by the surrounding aqueous medium and has been coated on the polished surface. The coupling efficiency has been maximized between the fundamental core guided mode and the plasmon-polariton mode by creating the two sensing passageways near the polished surface, enabling the particular PCF-SPR sensor to achieve great sensitivity. The maximum achieved sensitivity for this PCF-SPR sensor in both spectral and amplitude interrogation methods are 216000 nm/RIU, 1680 RIU^{-1} , respectively. Maximum FOM was calculated 1200, and the resolution is 4.63×10^{-7} . A simple D-shaped PCF with five air holes having same diameter which exhibits such high sensitivity makes the proposed sensor standout in the field of PCF based SPR sensors. A detailed literature review in the relevant field indicates that the proposed sensor has achieved maximum sensitivity in the spectral interrogation method to date.

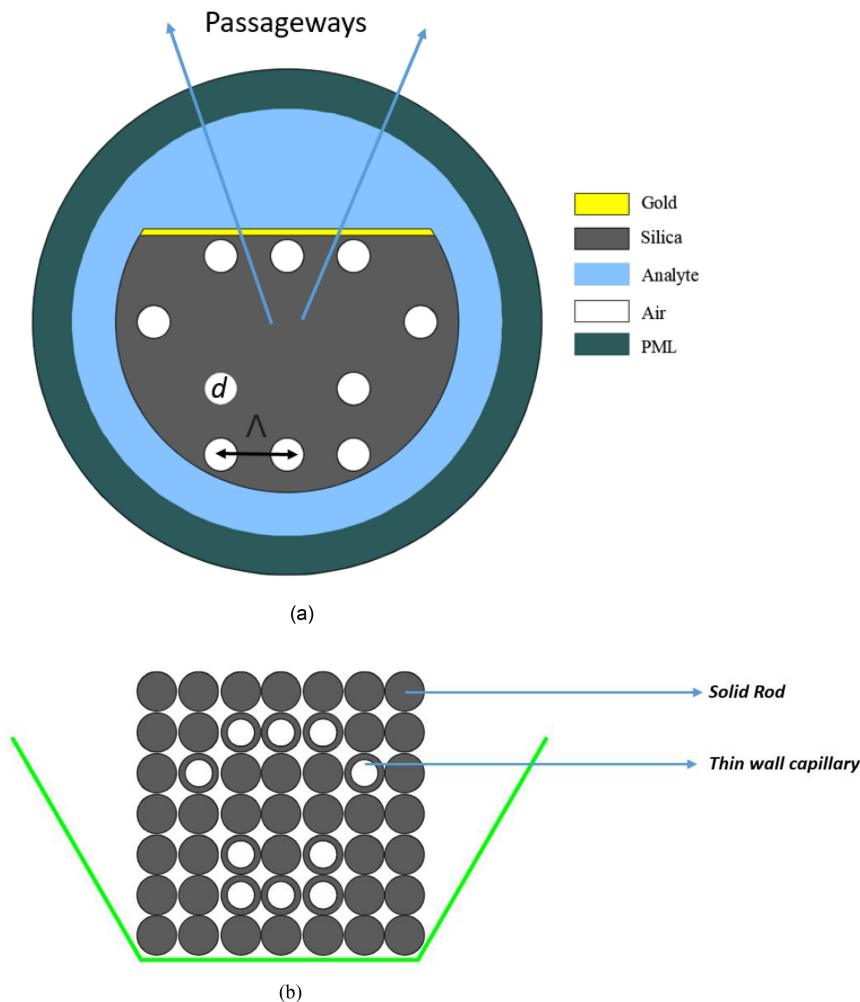


Fig. 1. (a) Proposed PCF-SPR sensor's 2D schematic diagram. (b) Fiber's fabrication arrangement.

2. Numerical Design and Modeling

The two-dimensional cross-section of the proposed sensor has been illustrated in Fig. 1(a). The structural design contains two layers of air hole ring having a square lattice setting. The center air hole and the three air holes from the first ring have been removed to create the proposed sensor's stable core. Three upper air holes from the 1st ring have been used to create isolation between the core and plasmonic material layer. Two upper corner side air holes from the 2nd ring have not been considered in the design to establish maximum efficiency of the coupling between fundamental core guided mode and plasmonic mode. The stack and draw method [5], [9], [19], also known as a state-of-the-art technique of fabricating PCF-SPR sensors, can be easily applied to fabricate the proposed sensor depicted in Fig. 1(b). All the solid rods and capillaries will be placed together, and then they will be lifted after a certain unit of a time period. During fabrication, solid rods with the same diameter and cylindrical capillaries having the same thickness will be used to create the no air hole and air holes of the proposed sensor. The fiber's D-shaped structure will be formed using the polishing technique mentioned in [5], [13]. Finally, the chemical deposition method will be followed to roof the plasmonic material gold on the polished surface of the proposed sensor [18], [19], [21].

Finite Element-based electromagnetic simulation software COMSOL Multiphysics (Version 5.4) has been used to investigate and analyze the proposed sensor's performances numerically. Extremely fine mesh was considered for simulation in order to achieve the maximum simulation accuracy. The primary structural parameters of the sensors such as air hole diameter (d), pitch (Λ), and thickness of plasmonic material (Au) have been optimized at $d = 1.65 \mu\text{m}$, $\Lambda = 3.30 \mu\text{m}$, and $\text{Au} = 80 \text{ nm}$, respectively. Drude-Lorentz model described in [Ref. [23] has been followed to calculate the refractive index of gold. The Sellmeier equation given following (1) has been considered to estimate the dielectric constant of SiO_2 (fused silica) used as the proposed sensor's background material.

$$n_{\text{SiO}_2}^2(\lambda) = 1 + \frac{B_1\lambda^2}{\lambda^2 - C_1} + \frac{B_2\lambda^2}{\lambda^2 - C_2} + \frac{B_3\lambda^2}{\lambda^2 - C_3} \quad (1)$$

Where n_{SiO_2} represents the refractive index of silica, λ indicates the wavelength of operation in μm , and B_n and C_n specify Sellmeier coefficients [$n = 1, 2, 3$].

3. Result and Discussion

The optical field distribution of the fundamental and plasmon-polariton modes has been illustrated in Figs. 2(a) and (b). In a photonic crystal fiber, air holes basically work as the cladding region. When light is transmitted, the whole optical field is confined within the core mode. On the contrary, plasmon polariton mode appears at the sensing medium where the plasmonic material has been coated. At the resonance condition, the wave vector of incident light of the core mode and surface plasmonic waves of the SPP mode gets equal with each other, which can also be defined as a phase-matching condition. The field distribution at surface plasmon resonance condition has also been depicted in Fig. 2(c). A noticeable amount of energy transfer has been observed at the phase-matching condition as the light energy gets absorbed by the plasmonic surface waves due to the establishment of strong energy coupling at the interface between the plasmonic material coating and dielectric medium. The dispersion relation of the 1st order core guided mode, 2nd order plasmon polariton mode, and the loss curve have been illustrated in Fig. 2(d). Since refractive index is a function of wavelength, effective index mode of SPP mode and fundamental mode change with wavelength. For the analyte value $\text{RI} = 1.33$, the indexes of refraction of the fundamental mode and the plasmon-polariton mode matched at the operating wavelength $1.49 \mu\text{m}$ as well as the establishment of strong coupling between these two modes occurred, which results in a sharp peak loss at the intersection point. For this specific PCF-SPR structure, it has been observed that the significant evanescent field has been produced due to the excitation of free electron of y-polarized transverse electric mode rather than the x-polarized transverse electric mode. And a significant amount of energy has been delivered from the core mode to plasmon polariton mode at the phase-matching condition.

The confinement loss calculation formula is given in the following equation [5], [21].

$$\alpha = \frac{40\pi \text{Im}(n_{\text{eff}})}{\ln(10)\lambda} \approx 8.686 \times k_0 \text{Im}(n_{\text{eff}}) \times 10^4 \text{ dB/cm} \quad (2)$$

Where denotes free space wave numbers, λ indicates the wavelength of operation in μm , and $\text{Im}(n_{\text{eff}})$ denotes the effective index's imaginary part.

The loss spectra for analyte RI range 1.23 to 1.42 at resonant wavelengths are illustrated in Fig. 3(a). Redshifting with propagation loss increased for the proposed PCF-SPR sensor as the incomplete coupling occurred while varying the value of RI to higher [18]. An excellent fitting agreement depicted in Fig. 3(b) has been observed from the polynomial fit curve of R- square value 0.98.

From (4) and (5) mentioned below, the spectral sensitivity and the resolution of the proposed PCF-SPR have been calculated [5], [10]. Maximum spectral sensitivity or WS of 216000 nm/RIU has been achieved, as well as resolution achieved 4.63×10^{-7} RIU while the analyte RI range varied from 1.23 to 1.42 having 0.01 step size. And the maximum wavelength sensitivity has been

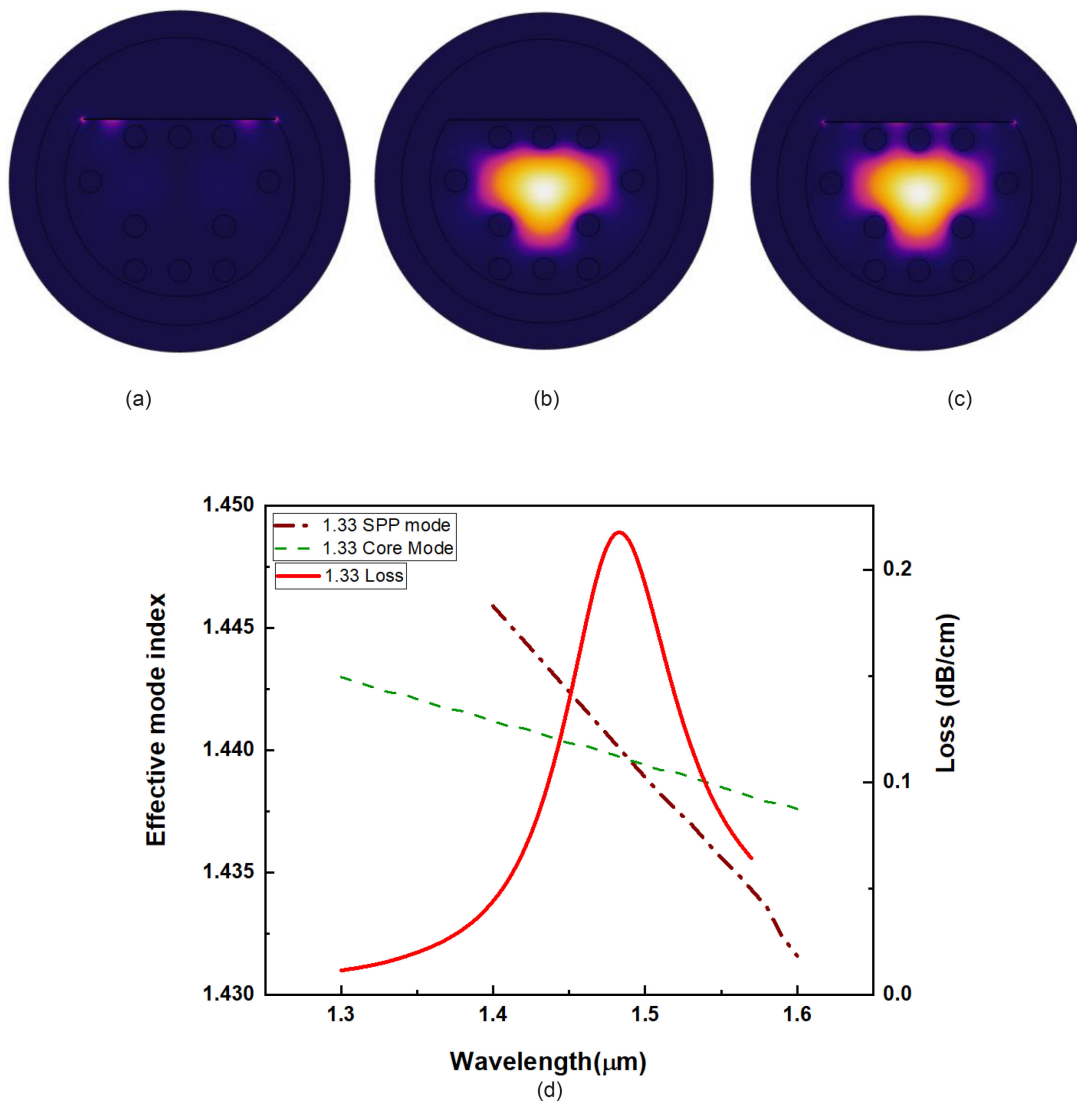
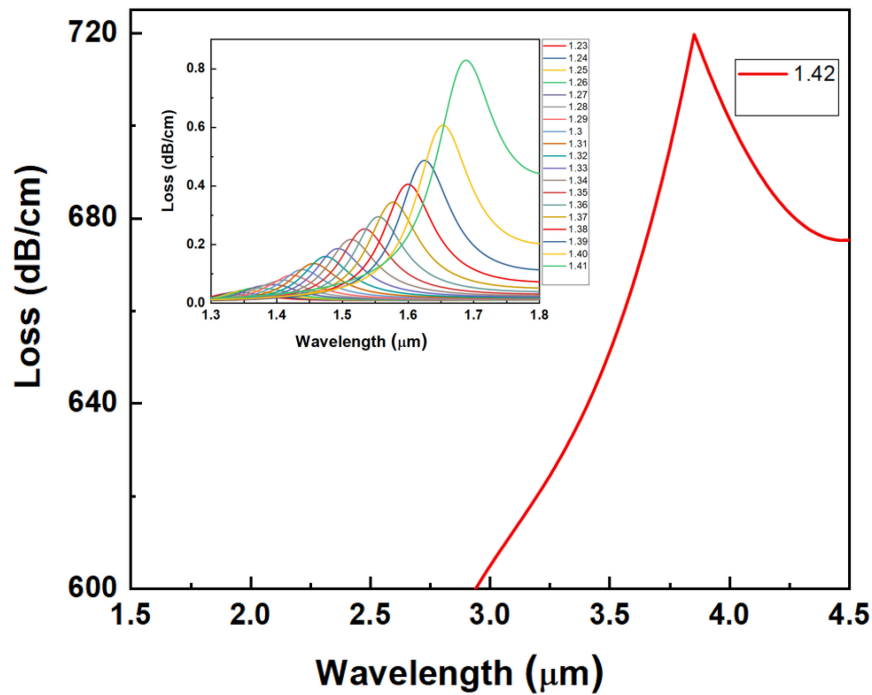


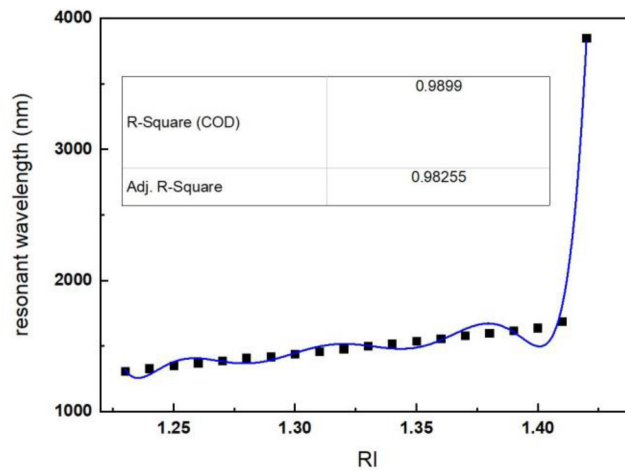
Fig. 2. Light field distribution for RI = 1.33. (a) Plasmon polariton mode. (b) Fundamental core guided mode. (c) SPR condition. (d) Dispersion relations of the fundamental mode and plasmonic mode.

observed when the analyte value was changed from 1.23- to 1.40. The wavelength sensitivities of the proposed PCF-SPR for the analyte range 1.23 to 1.41 are 1000,1000,2000, 2000, 2000, 2000, 2000, 2000, 2000, 2000, 2000, 2000, 2000, 2000, 2000, 2000, 2000, 7000 and 216000 nm/RIU, respectively. At resonant wavelength 1320 nm, the minimum loss of 0.03 dB/cm has been observed, where the maximum loss of 720 dB/cm occurred at 3850m wavelength. Furthermore, the establishment of extremely strong coupling between the core and plasmon-polariton modes leads to high propagation loss at analyte RI 1.42. Additionally, the proposed sensor shows a maximum FOM (Figure of Merit = Sensitivity/FWHM) [25] of 1200, where the minimum achieved FOM is 10 for analyte value 1.41 and 1.23, respectively.

$$WS[nm/RIU] = \frac{\Delta\lambda_{\text{peak}}}{\Delta n_a} \quad (3)$$



(a)



(b)

Fig. 3. (a) Propagation loss curves of the proposed PCF-SPR sensor for analytes RI range 1.23 to 1.42. (b) Resonant wavelengths' polynomial curve fitting.

Where $\Delta\lambda_{\text{peak}}$ expresses resonance peak shifting of loss curves, and Δn_a indicates a step size of varying analyte RI.

$$R = \Delta n_a \Delta\lambda_{\text{min}} / \Delta\lambda_{\text{peak}} RIU \tag{4}$$

Where $\Delta\lambda_{\text{min}}$ denotes the resolution of minimum wavelength, and $\Delta\lambda_{\text{peak}}$ expresses resonance peak shifting of loss curves in the wavelength domain.

The structural parameters of the proposed PCF-SPR, such as air hole diameter, pitch, and plasmonic material thickness, have been varied. Their impacts toward sensitivity on the resonant

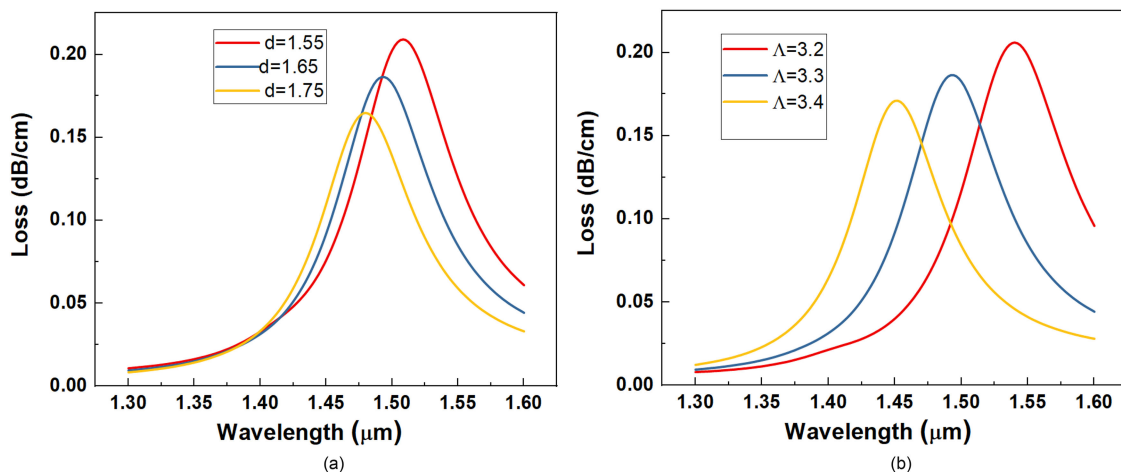


Fig. 4. Confinement loss curves for different value of (a) d , (b) Pitch Δ .

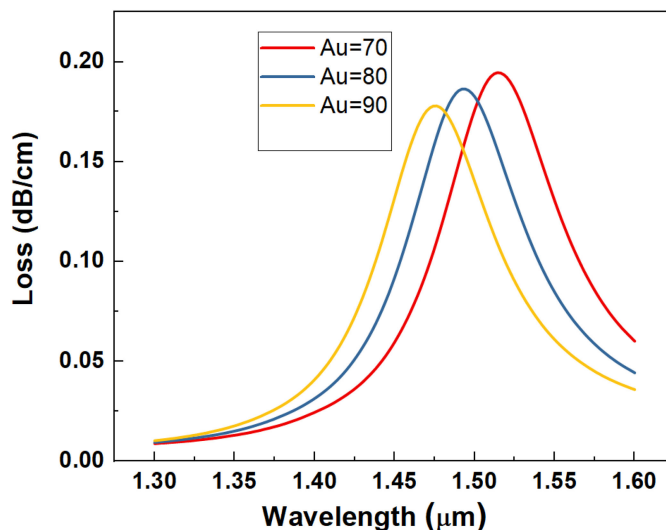


Fig. 5. Confinement loss curves for different value of Au.

wavelength have been investigated. The performances showed at different structural parametric values have been illustrated in Fig. 4 and Fig. 5.

Fig. 4(a) shows that blueshifting occurs while tuning the value of d from $1.55 \mu\text{m}$ to $1.75 \mu\text{m}$ with propagation loss being decreased. This has happened as the coupling strength between the core and plasmon-polariton modes are getting weaker with the increasing value of d . This results in comparatively less amount of energy transfer from the core mode to SPP mode and vice-versa. Similarly, in Fig. 4(b), while varying the pitch value from 3.2 to $3.4 \mu\text{m}$, a noticeable blue shift is observed with confinement loss being decreased due to weak coupling.

The significance of the thickness of plasmonic material gold (Au) on loss curves has been shown in Fig 5. It is seen that significant blueshifting is observed while tuning the thickness value of Au from 70 nm to 90 nm . This behavior from the proposed PCF-SPR is shown as the refractive index of the surrounding medium of fundamental core guided mode. The plasmon polariton mode changes with the changing value of Au thickness [8]. For that reason, the phase matching point is

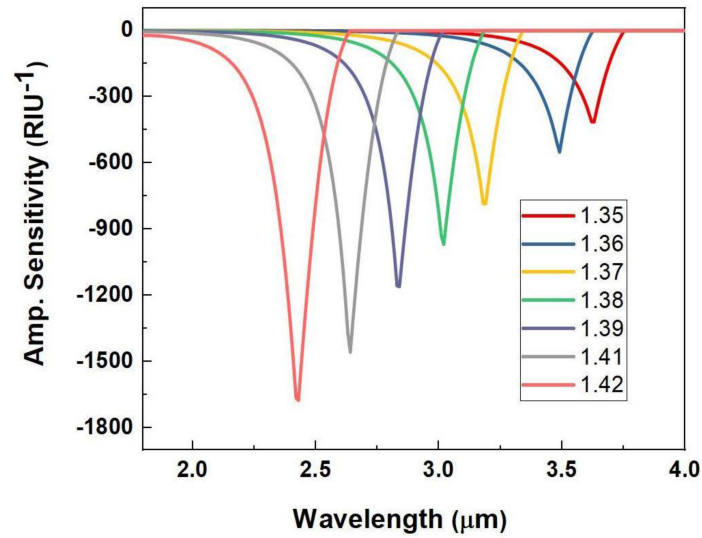


Fig. 6. Amplitude sensitivity (AS) of the proposed PCF-SPR sensor for analytes RI range 1.34 to 1.39.

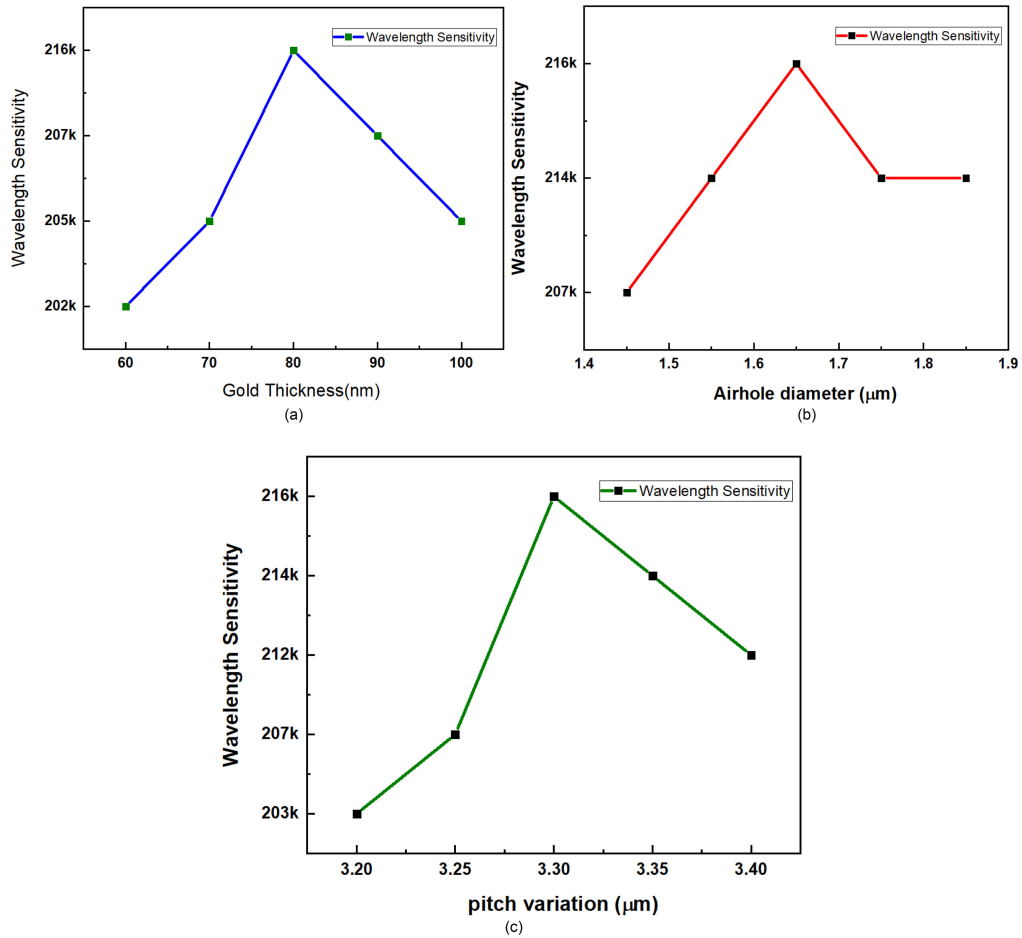


Fig. 7. Spectral sensitivity or wavelength sensitivity (WS) for different value of (a) Gold thickness (b) Airhole diameter (c) Pitch value.

TABLE 1
Comparison of Performances of the Proposed PCF-SPR Sensor With Recent Reported PCF-SPR Sensors

Parameter	Tolerance (%)	Wavelength sensitivity
Airhole diameter	-2	215,950
	0	216,000
	2	215,980
Pitch	-2	215,985
	0	216,000
	2	215,965
Gold Thickness	-2	215,990
	0	216,000
	2	215,995

TABLE 2
Comparison of Performances of the Proposed PCF-SPR Sensor With Recent Reported PCF-SPR Sensors

Ref.	Max. WS	Max. AS	Lowest. R	Max. FOM	RI Range
[5]	46,000	1086	2.2×10^{-6}	—	1.33-1.43
[13]	31,000	--	3.31×10^{-5}	—	1.32-1.40
[14]	62,000	1415	1.6×10^{-6}	1140	1.33-1.43
[21]	51,000	1872	1.96×10^{-6}	566	1.22-1.37
[26]	17000	74	5.8×10^{-6}	—	—
[27]	5200	--	1.92×10^{-5}	—	1.33-1.37
[28]	11000	631	9.09×10^{-6}	157	1.33- 1.40
[29]	50000	1449	2×10^{-6}	—	—
[30]	111000	2050	9×10^{-7}	—	1.33-1.43
Proposed	216000	1680	4.63×10^{-7}	1200	1.23-1.42

also getting changed to lower wavelengths. Propagation loss decreases as the coupling strength between the core and plasmon polaritons are weaker. Finally, the optimized value for Au thickness was determined by 80 nm after investigation.

The proposed PCF-SPR sensor's amplitude sensitivity has been calculated from the [Ref. [5] and given following in (5). It has been found that the sensor shows maximum and minimum AS of 1680 and 20 RIU-1 for analyte value $n_a = 1.42$ and $n_a = 1.23$, respectively. Fig. 6 illustrates the AS

of the proposed sensor for analyte RI range 1.35 to 1.42.

$$AS[RIU^{-1}] = -\frac{1}{\alpha(\lambda, n_a)} \frac{\partial \alpha(\lambda, n_a)}{\partial n_a} \quad (5)$$

Where $\alpha(\lambda, n_a)$, expresses the confinement loss for the selected analyte RI, the variance between two confinement loss curves is expressed by $\partial \alpha(\lambda, n_a)$, and step size of varying analyte RI is indicated by ∂n_a .

The impact of varying the thickness of plasmonic material gold, air hole diameter, and pitch value toward wavelength sensitivity have been depicted in Fig. 7(a), (b), and (c), respectively. It has been observed that the highest WS of 216000 nm/RIU has been achieved for the proposed sensor having an Au thickness value of 80 nm, an air diameter d value of 1.65 μm , and a pitch value of 3.3 μm . Therefore, these values have been selected as optimized values for the proposed sensor. Moreover, with the current state of the art fabrication technology [14] maximum $\pm 2\%$ fabrication tolerances has been considered which is shown in Table 1. It is clearly visible that the $\pm 2\%$ fabrication errors has negligible effects on the wavelength sensitivity of the proposed sensor.

The proposed sensor's performance parameters are tabulated in Table 2 and compared with other recent reported PCF-SPR sensors. After a detailed comparison, it has been found that the proposed sensor has shown the highest WS sensitivity, highest FOM, lowest resolution among all recently reported sensors mention in Table 2.

4. Conclusion

An extremely sensitive PCF-SPR sensor was proposed in this work for the analyte refractive index detection range 1.23 to 1.42. The coupling efficiency was maximized between the fundamental core guided mode and the plasmon-polariton mode by creating the two external sensing passageways near the polished surface, enabling the particular PCF-SPR sensor to achieve great sensitivity. Numerical investigation exhibited that the proposed sensor has a maximum WS of 216,000 nm/RIU, highest among other recently reported PCF-SPR sensors. The proposed sensor also showed maximum AS, resolution, and FOM of 1680 RIU⁻¹, 4.62×10^{-7} , and 1200, respectively. Furthermore, the external sensing mechanism makes the proposed sensor robust and feasible for practical implementation. Hence the proposed sensor can be a suitable candidate in the field of biomedical sensing, chemical sensing, and so on.

References

- [1] Y. Zhan *et al.*, "Surface plasmon resonance-based microfiber sensor with enhanced sensitivity by gold nanowires," *Opt. Mater. Exp.*, vol. 8, no. 12, pp. 3927–3940, 2018.
- [2] M. R. Hasan, S. Akter, K. Ahmed, and D. Abbott, "Plasmonic refractive index sensor employing niobium nanofilm on photonic crystal fiber," *IEEE Photon. Technol. Lett.*, vol. 30, pp. 315–318, Feb. 2018.
- [3] G. An, S. Li, H. Wang, X. Zhang, and X. Yan, "Quasi-D-shaped optical fiber plasmonic refractive index sensor," *J. Opt.*, vol. 20, no. 3, 2018.
- [4] J. Lu, Y. Li, Y. Han, Y. Liu, and J. Gao, "D-shaped photonic crystal fiber plasmonic refractive index sensor based on gold grating," *Appl. Opt.*, vol. 57, no. 19, pp. 5268–5272, 2018.
- [5] A. A. Rifat, R. Ahmed, G. Amouzad Mahdiraji, and F. R. M. Adikan, "Highly sensitive D-Shaped photonic crystal fiber-based plasmonic biosensor in visible to Near-IR," *IEEE Sensors J.*, vol. 17, pp. 2776–2783, May 2017.
- [6] G. An, X. Hao, S. Li, X. Yan, and X. Zhang, "D-shaped photonic crystal fiber refractive index sensor based on surface plasmon resonance," *Appl. Opt.*, vol. 56, no. 24, pp. 6988–6992, Aug. 2017.
- [7] K. S. Patnaik and R. Jha, "Graphene-based conducting metal oxide coated d-shaped optical fiber spr sensor," *IEEE Photon. Technol. Lett.*, vol. 27, no. 23, pp. 2437–2440, 2015.
- [8] N. Luan, R. Wang, W. Lv, and J. Yao, "Surface plasmon resonance sensor based on D-shaped microstructured optical fiber with hollow core," *Opt. Exp.*, vol. 23, no. 7, pp. 8576–8582, 2015.
- [9] A. Kumar Paul, A. Krishno Sarkar, A. B. S. Rahman, and A. Khaleque, "Twin core photonic crystal fiber plasmonic refractive index sensor," *IEEE Sensors J.*, vol. 18, no. 14, pp. 5761–5769, Jul. 2018.
- [10] M. R. Hasan *et al.*, "Spiral photonic crystal fiber-based dual-polarized surface plasmon resonance biosensor," *IEEE Sensors J.*, vol. 18, no. 1, pp. 133–140, Jan. 2018.
- [11] J. N. Dash, R. Das, and R. Jha, "AZO coated microchannel incorporated PCF-Based SPR sensor: A numerical analysis," *IEEE Photon. Technol. Lett.*, vol. 30, no. 11, pp. 1032–1035, 2018.

- [12] M. Liu, X. Yang, P. Shum, and H. Yuan, "High-sensitivity birefringent and single-layer coating photonic crystal fiber biosensor based on surface plasmon resonance," *Appl. Opt.*, vol. 57, pp. 1883–1886, 2018.
- [13] J. Wu, S. Li, X. Wang, M. Shi, X. Feng, and Y. Liu, "Ultra-high sensitivity refractive index sensor of a D-shaped PCF based on surface plasmon resonance," *Appl. Opt.*, vol. 57, no. 15, pp. 4002–4007, 2018.
- [14] M. Islam *et al.*, "Dual-polarized highly sensitive plasmonic sensor in the visible to near-IR spectrum," *Opt. Exp.*, vol. 26, no. 23, pp. 30347–30361, 2018.
- [15] T. Bellunato, M. Calvi, C. Matteuzzi, M. Musy, D. L. Perego, and B. Storaci, "Refractive index of silica aerogel: Uniformity and dispersion law," *Nucl. Instr. Met. Phys. Re.*, vol. 595, pp. 183–186, 2008.
- [16] F. Wang, C. Liu, Z. Sun, T. Sun, B. Liu, and P. K. Chu, "A highly sensitive SPR sensor based on two parallel PCFs for low refractive index detection," *IEEE Photon. J.*, vol. 10, no. 4, Aug. 2018, Art. no. 7104010.
- [17] C. Liu *et al.*, "Birefringent PCF-Based SPR sensor for a broad range of low refractive index detection," *IEEE Photon. Technol. Lett.*, vol. 30, no. 16, pp. 1471–1474, Aug. 2018.
- [18] X. Chen, L. Xia, and C. Li, "Surface plasmon resonance sensor based on a novel D-Shaped photonic crystal fiber for low refractive index detection," *IEEE Photon. J.*, vol. 10, no. 1, Feb. 2018, Art. no. 6800709.
- [19] E. Haque, M. A. Hossain, F. Ahmed, and Y. Namihira, "Surface plasmon resonance sensor based on modified D-Shaped photonic crystal fiber for wider range of refractive index detection," *IEEE Sensors J.*, vol. 18, no. 20, pp. 8287–8293, Oct. 2018.
- [20] C. Liu *et al.*, "Mid-infrared surface plasmon resonance sensor based on photonic crystal fibers," *Opt. Exp.*, vol. 25, no. 13, pp. 14227–14237, 2017.
- [21] E. Haque, M. Anwar Hossain, Y. Namihira, and F. Ahmed, "Microchannel-based plasmonic refractive index sensor for low refractive index detection," *Appl. Opt.*, vol. 58, no. 6, pp. 1547–1554, 2019.
- [22] M. A. Hossain and Y. Namihira, "Center wavelength adoption techniques for supercontinuum generating highly nonlinear noncircular core photonic crystal fiber," *Jpn. J. Appl. Phys.*, vol. 52, no. 5R, 2013, Art. no. 052502.
- [23] S. Jiao, S. Gu, H. Yang, H. Fang, and S. Xu, "Highly sensitive dual-core photonic crystal fiber based on a surface plasmon resonance sensor with a silver nano-continuous grating," *Appl. Opt.*, vol. 57, no. 28, pp. 8350–8358, 2018.
- [24] M. A. Hossain *et al.*, "Tailoring supercontinuum generation using highly nonlinear photonic crystal fiber," *Opt. Laser Technol.*, vol. 44, no. 6, pp. 1889–1896, 2012.
- [25] A. K. Mishra, S. K. Mishra, and B. D. Gupta, "SPR based fiber optic sensor for refractive index sensing with enhanced detection accuracy and figure of merit in visible region," *Opt. Commun.*, vol. 344, pp. 86–91, 2015.
- [26] J. N. Dash, "Highly sensitive side-polished birefringent PCF-Based SPR sensor in near IR," *Plasmonic*, vol. 11, no. 6, pp. 1505–1509, 2016.
- [27] J. N. Dash and R. Jha, "Highly sensitive d shaped PCF sensor based on SPR for near IR," *Opt. Quantum Electron.*, vol. 48, no. 137, 2016.
- [28] F. Haider, M. Mashrafi, R. Haider, R. A. Aoni, and R. Ahmed, "Asymmetric core-guided polarization-dependent plasmonic biosensor," *Appl. Opt.*, vol. 59, no. 26, pp. 7829–7835, 2020.
- [29] M. A. Mollah and M. S. Islam, "Novel single hole exposed-suspended core localized surface plasmon resonance sensor," *IEEE Sensors J.*, vol. 21, no. 3, pp. 2813–2820, Feb. 2021.
- [30] M. S. Islam *et al.*, "Localized surface plasmon resonance biosensor: An improved technique for SERS response intensification," *Opt. Lett.*, vol. 44, no. 5, pp. 1134–1137, 2019.
- [31] E. Haque, S. Mahmuda, M. A. Hossain, N. H. Hai, Y. Namihira, and F. Ahmed, "Highly sensitive dual-core PCF based plasmonic refractive index sensor for low refractive index detection," *IEEE Photon. J.*, vol. 11, no. 5, Oct. 2019, Art. no. 7905309.